Dyes and Pigments 173 (2020) 107888

Contents lists available at ScienceDirect

Dyes and Pigments

journal homepage: www.elsevier.com/locate/dyepig

Dansyl-peptide dual-functional fluorescent chemosensor for Hg^{2+} and biothiols

Xuliang Pang[a], Jianfang Dong[a], Lei Gao[b], Lei Wang[a], Shuaibing Yu[a], Jinming Kong[c], Lianzhi Li[a,*]

[a] School of Chemistry and Chemical Engineering, Liaocheng University, Liaocheng, 252059, China
[b] Zhong Yuan Academy of Biological Medicine, Liaocheng People's Hospital, Liaocheng, 252000, China
[c] School of Environmental and Biological Engineering, Nanjing University of Science and Technology, 200 Xiaolingwei, Nanjing, 210094, China

ARTICLE INFO

Keywords:
Peptide chemosensor
FRET
Mercury ion
Biothiols

ABSTRACT

A new dansyl-peptide dual-functional fluorescent chemosensor (D-ECEW-NH_2, D-P4) was developed via Fmoc solid phase peptide synthesis (SPPS), which displayed an excellent selectivity and high sensitivity for Hg^{2+} by turn on response in 10 mM 2-[4-(2-Hydroxyethyl)-1-piperazinyl]ethanesulfonic acid (HEPES) solution (pH 7.1). The sensing mechanism for Hg^{2+} is by two pathways, one is fluorescence resonance energy transfer (FRET) effect between tryptophan (donor) and dansyl (acceptor) fluorophores due to the interaction of Hg^{2+} ion with D-P4 evidenced by fluorescence excitation spectra at 290 nm, while the other is the chelation enhanced fluorescence (CHEF) effect evidenced by fluorescence excitation spectra at 330 nm. D-P4 sensor was used to detect Hg^{2+} with low detection limit of 23.0 nM. Furthermore, the binding stoichiometry and binding constant, as well as pH influence of D-P4 for Hg^{2+} were investigated. Surprising but interestingly, D-P4-Hg system has been found a significant fluorescence enhancement response toward biothiols including cysteine (Cys), homocysteine (Hcy) and glutathione (GSH), which can be used for the detection of biothiols. Its detection limit for Cys was 52.0 nM.

1. Introduction

Metallic ion detection is crucial because of its significance in biological, environmental, chemical, and medical fields [1,2]. Among various heavy and transition metal (HTM) ions, Hg^{2+} was seen as one of the most hazardous and toxic environmental pollutants with grisly immunotoxic, neurototoxic, and genotoxic effects [3,4]. Excess accumulation of Hg^{2+} and its derivatives in humans can lead to a series of severe diseases, such as motor and cognitive disorders, kidney failure, central nervous system damage and even death [5]. Allowable Hg^{2+} level in drinking water is 10 nM according to the United States Environmental Protection Agency (USEPA) [6]. Therefore, the detection of Hg^{2+} is of great significance.

Recently, various fluorescent chemosensors for heavy metal ions detection have been reported, some of them are complicated and difficult to synthesize [7–12]. Table 1 lists some recent reports of fluorescent chemosensors for the determination of Hg^{2+} [13–26]. Additionally, several Hg^{2+} sensitive sensors usually showed low selectivity due to interference from other metal ions (such as Ag^{+}, Cu^{2+}, and Cd^{2+} ions) [27]. By contrast, the peptide based fluorescent chemosensor for Hg^{2+} exhibits excellent selectivity, high sensitivity, and good water solubility. Peptide based fluorescent chemosensors have their own advantages [28]: matured solid-phase peptide synthesis technology; tunable selectivity and sensitivity of sensors through peptide backbone; variable recognition mode such as fluorescence resonance energy transfer (FRET), photoinduced electron transfer (PET) and chelation enhanced fluorescence (CHEF) [29,30]; peptide based chemosensors are superior to organic sensors due to their low toxicity, high water solubility and biocompatibility. Therefore, peptide fluorescent chemosensors have been widely used in metal ion detection, biomacromolecule detection, bioimaging research, medical diagnosis and treatment [31–37].

Based on these advantages, we designed and synthesized a dansyl-peptide (D-ECEW-NH_2, D-P4) chemosensor for Hg^{2+}. This chemosensor contains a tryptophan residue (donor) and a dansyl (receptor) fluorophore, which possesses both a donor moiety and a receptor moiety to realize the sensing of Hg^{2+} ion by two different mechanisms including FRET and CHEF.

Among various chemosensors for metallic ions, only a few of chemosensors have multi-functional recognition based on the coordination complex between the first analyte and host molecule [38].

Intracellular biothiols including glutathione (GSH), cysteine (Cys) and homocysteine (Hcy) play important biological roles in cellular metabolism and maintaining cellular redox homeostasis via their free

* Corresponding author. No. 1, Hunan Road, Liaocheng, 252059, PR China.
E-mail address: lilianzhi1963@163.com (L. Li).

https://doi.org/10.1016/j.dyepig.2019.107888
Received 14 June 2019; Received in revised form 31 August 2019; Accepted 15 September 2019
Available online 16 September 2019
0143-7208/

Table 1
Various spectroscopic sensing systems for determination of Hg^{2+}.

Method	System	LOD	Reference
Fluorescence	Chemosensor based on Schiff-base	22.68 nM	13
Fluorescence	Naphthalene anhydride and imidazole-type sensor	16 nM	14
Fluorescence	Dansyl-P23	1.4 μM	15
Fluorescence	Perylene-bisimide sensor	2.2 μM	16
Fluorescence	Cyclam derivative	7.9 μM	17
Fluorescence	A squaraine-bis(rhodamine-B) derivative	6.48 μM	18
Fluorescence	Rhodamine B derivative	50 nM	19
Fluorescence	Fluorescein connected with rhodamine B fluorophores	20.2 nM	20
Fluorescence	Rhodamine derivative	120 nM	21
Fluorescence	NBD–CC–NBD	25.6 nM	22
Fluorescence	*N*-[*p*-(dimethylamino)benzamido]-*N*′-phenylthiourea	39.0 nM	23
Fluorescence	Dansyl-AACAAHCWAE	25.9 nM	24
Fluorescence	Pyr-Y	12 nM	25
Fluorescence	Rhodamine 6G-based Chemosensor	170 nM	26
Fluorescence	Dansyl-ECEW-NH_2	23.0 nM	This work

thiols [39]. GSH, an important tripeptide, play very important roles in human body, change of cellular GSH level is associated with several diseases, such as leucocyte loss, HIV infection and liver damage [40]. Among biological thiols, Cys has various vital biological functions in human body, for example in detoxification and protein metabolism. Some neurological diseases, such as Parkinson's disease and Alzheimer's disease were also connected with the abnormalities of Cys [41]. Hcy is a variant of cysteine with a structure similar to Cys, its level is considered as one of the important parameter for cardiovascular disease and Alzheimer's disease [42]. Due to various important biological functions of biothiols in biological systems, fast and efficient detection method for sensing and quantification of the level of biothiols in different samples (environmental, cellular, and medicine) is imperative in biochemistry. Scheme 1 is the proposed binding mode of D-P4 with Hg^{2+} and biothiols.

2. Experimental

2.1. Reagents and instruments

Fmoc-Rink Amide AM Resin (0.57 mmol/g) and Fmoc protected amino acids (Fmoc-L-Glu(OtBu)-OH, Fmoc-L-Cys(Acm)-OH, and Fmoc-L-Trp(Boc)-OH) were purchased from C S Bio. Co., USA. Dansyl chloride was obtained from Shanghai Macklin Biochemical Co., Ltd. N,N-diisopropylethyla (DIEA), tri-isopropylsilane (TIS), Trifluoroacetic acid (TFA) and 2-(1H-benzotriazole-1-yl)-1,1,3,3-tetramethyluronium hexafluorophosphate (HBTU) were gained from Shanghai GL Biochem Ltd. Amino acids, homocysteine (Hcy) and glutathione (GSH) were purchased from Sigma Chemical Co. Ltd. All other chemicals used were of analytical reagent grade unless otherwise noted. Stock solutions of the various metal salts were prepared with 10 mM HEPES buffer (pH 7.1),

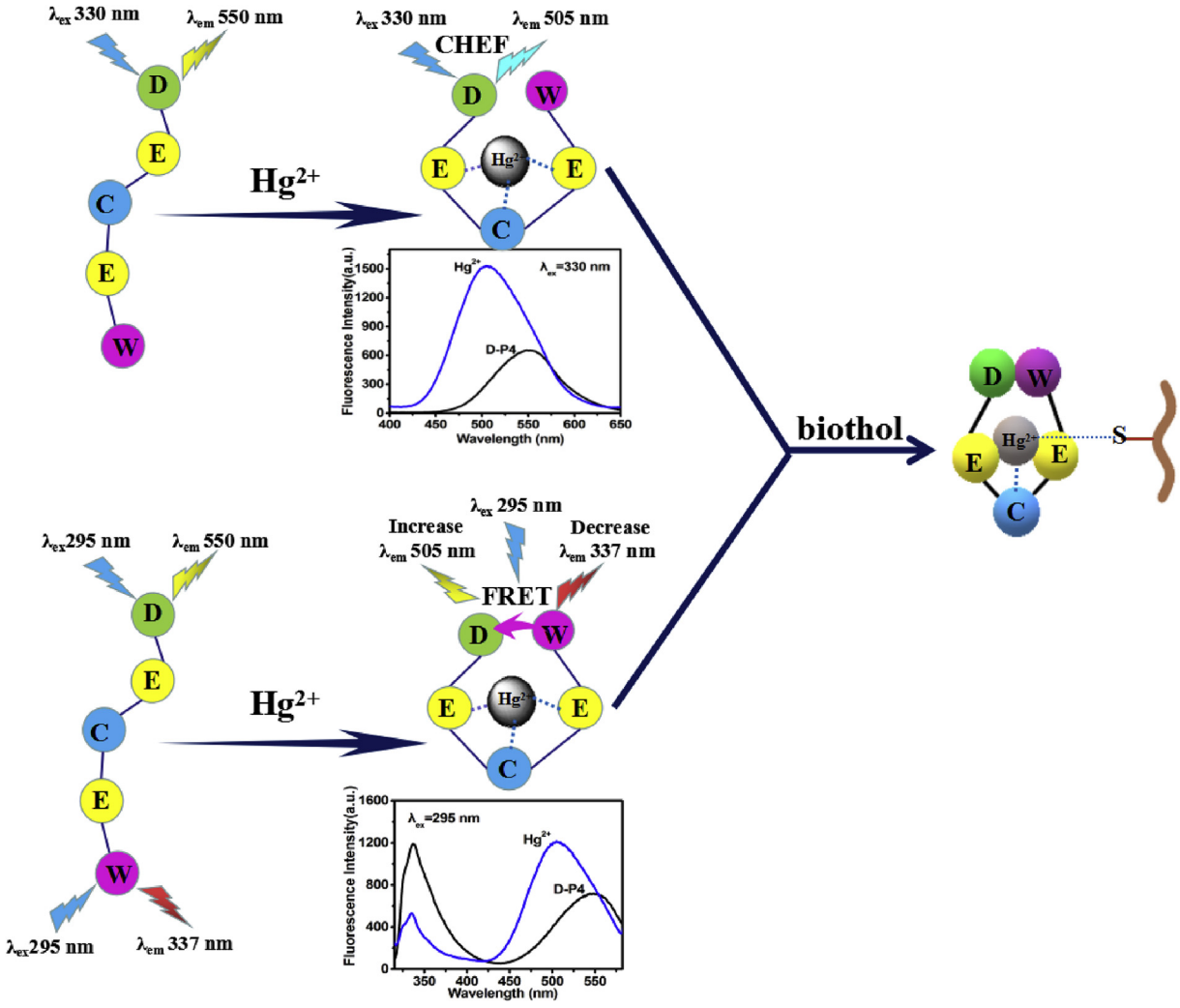

Scheme 1. Proposed binding mode of D-P4 with Hg^{2+} and biothiols.

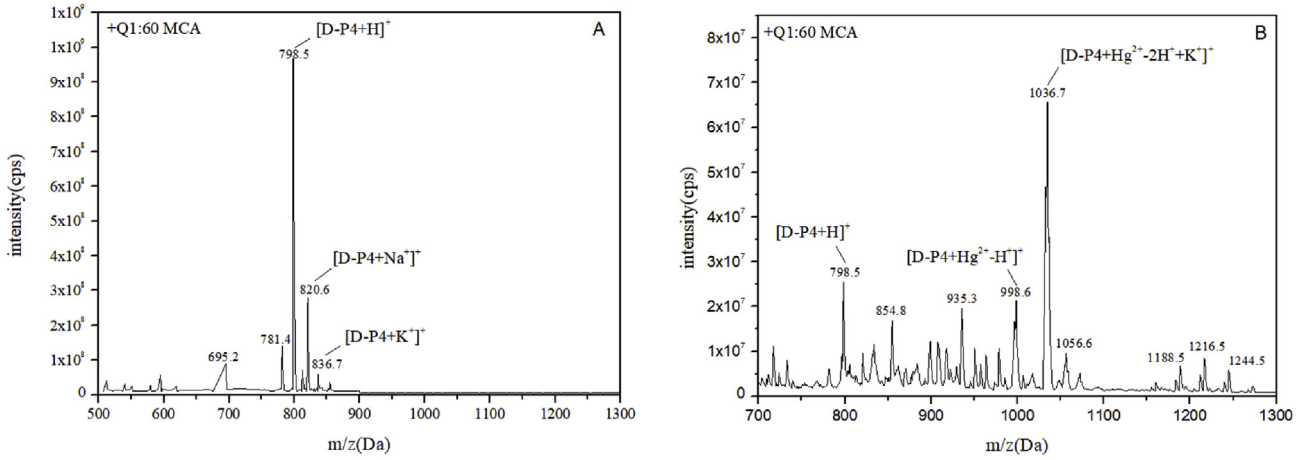

Fig. 1. ESI mass spectrum of D-P4 (10.0 μM) (A) and D-P4-Hg (10.0 μM) (B) in EtOH:H_2O (1:1) solutions.

which were used throughout the study.

CS 136 Peptide Synthesizer (CS Bio Co., USA); Hitachi F-7000 spectrofluorometer (Hitachi Inc., Japan); Lambda 750 spectrophotometer (PerkinElmer, USA); High Performance Liquid Chromatography (HPLC) system (model 426 HPLC pump, UVIS 201 detector, Alltech, USA); API 4500 QTRAP Mass Spectrometer (Applied Biosystems/MDS SCIEX, USA). Nicolet 5700 Fourier transform spectrometer (Thermo Electron Corporation, USA). ESCALAB Xi + X-ray photoelectron spectroscopy (XPS) (Thermo Fisher Scientific Inc, USA). Bruker AVANCE NEO 500 MHz spectrometer. FLS 1000 Photoluminescence Spectrometer (UK).

2.2. Preparation of D-P4

Dansyl-Glu-Cys-Glu-Trp-NH_2 (D-P4) was prepared via solid phase peptide synthesis (SPPS) technology. Activated Fmoc-L-Trp-OH (1.8 mM) using HBTU (1.8 mM) and DIEA (1.8 mM) was connected with Rink Amide AM Resin (0.6 mM). The Fmoc group was then deprotected, followed by the assembly of Fmoc-L-Glu(OtBu)-OH (1.8 mM), Fmoc-L-Cys(Acm)-OH (1.8 mmol), and Fmoc-L-Glu(OtBu)-OH (1.8 mM), successively. To the resin bound tetrapeptide, dansyl chloride (1.8 mmol) in DMF was added. Then, the resin was dried by pumps after being washed with DMF (30 mL), DCM (30 mL) and methanol (30 mL), three times respectively. The peptide was obtained by cleavage from Rink Amide AM Resin treated with a mixture of 18.5 mL TFA:Thioanisole:Phenol:H_2O:EDT (82.5:5:5:5:2.5, v/v/v/v/v) in a dark room at room temperature for 4 h. The crude peptide was precipitated in ice-cold ether and then centrifuged at 8000 rpm for 5 min at 4 °C, multiple washings and centrifugations, finally freeze-dried. The obtained crude peptide was analyzed and purified by a high performance liquid chromatography (HPLC) using C18 column. Mobile phase A is 0.1% TFA and 80% CH_3CN, mobile phase B is 0.1% TFA. ESI mass spectrometry was operated in positive ion mode with the operating parameters: the electrospray voltage was set to 5500 V; curtain gas, 20 psi; GS 1, 45 psi; GS 2, 50 psi. Temperature: 500 °C. Nitrogen was used as neulizer and desolvation gas.

2.3. General spectroscopy measurements

1.5 mM D-P4 stock solution was prepared in 10 mM HEPES buffer solution (pH 7.1) and stored at cold and dark room. All spectral measurements used this stock solution after appropriate dilution. Fluorescence spectra were measured using a 1 cm path length quartz cuvette at excitation wavelength of 330 nm and 295 nm, respectively. Slit widths of 5 nm were used for both excitation and emission. Fluorescence spectra of D-P4 were measured in the absence and presence of 17 metal ions (Na^+, Mg^{2+}, Al^{3+}, K^+, Ca^{2+}, Cr^{3+}, Mn^{2+}, Fe^{3+}, Co^{2+}, Zn^{2+}, Pb^{2+}, Cd^{2+}, and Hg^{2+} as chloride salts, Fe^{2+} as sulfate salt, Ni^{2+}, Cu^{2+} as acetate salts and Ag^+ as nitrate salt) and 9 anions ($NaNO_3$, Na_2SO_4, Na_3PO_4, $NaClO_4$, NaAc, KF, NaCl, KBr, and KI) in 10 mM HEPES buffer solution at pH 7.1

The fluorescence lifetime experiment was performed by a time-dependent single-electron counting method using a pulsed xenon lamp as a light source with an excitation wavelength of 295 nm and emission wavelengths of 337 nm and 505 nm, respectively. The fitting formula for fluorescence lifetime is given by the instrument: $R(t) = B_1e^{(-t/\tau1)} + B_2e^{(-t/\tau2)}$; $R(t) = B_1e^{(-t/\tau1)} + B_2e^{(-t/\tau2)} + B_3e^{(-t/\tau3)}$. Fluorescence lifetime can be obtained by formula $\mathbf{[\tau]} = \Sigma\tau_iB_i$. The quality of the fit can be determined by χ^2 value.

2.4. pH influence on fluorescence spectra

The fluorescence spectra of D-P4, D-P4-Hg system were measured at different pH solution with the excitation of 330 nm. The pH value of the sample solution was adjusted by appropriate additions of $HClO_4$ or NaOH solution.

2.5. Fluorescence response of D-P4-Hg to biothiols

Fluorescence spectra of D-P4-Hg in the presence of GSH, Hcy, Cys and other 19 amino acids were measured in 10 mM HEPES buffer solution at pH 7.1 with the excitation of 330 nm. Slit widths of 5 nm were used for both excitation and emission.

3. Results and discussion

3.1. Solid phase synthesis of D-P4

Dansyl-Glu-Cys-Glu-Trp-NH_2 (D-P4) was efficiently prepared via SPPS using Fmoc-chemistry. After cleavage of the product from Rink Amide AM Resin, D-P4 was purified from crude product by semi-preparative HPLC with a C18 column. The successful synthesis was confirmed by ESI mass spectrometer (Fig. 1). ESI mass of D-P4 is calculated as 798.25 [M + H^+]. Observed 798.5 as [M + H^+], 820.2 as [M + Na^+]$^+$ and 836.7 as [M + K^+]$^+$ (Fig. 1A). Fig. 1B showed the ESI MS results of D-P4-Hg, we found the occurrences of peak 998.6 and 1036.7 correspond to [D-P4 + Hg^{2+}–H^+]$^+$ and [D-P4 + Hg^{2+}–2H^+ + K^+]$^+$, respectively. At the same time, the peak intensity of 798.5 is significantly lower than in Fig. 1 A. These results confirmed that D-P4 could bind Hg^{2+} in the ratio of 1:1.

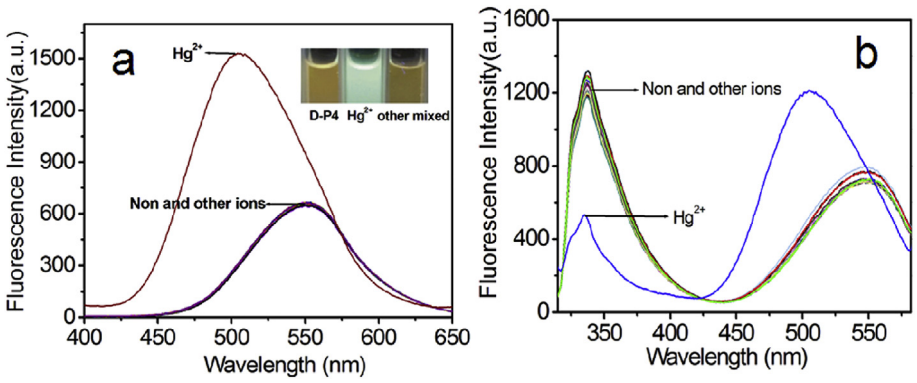

Fig. 2. Fluorescence spectra of D-P4 (20.0 μM) in the presence of 17 metal ions and 9 anions with excitation wavelength of 330 nm (**a**) and 295 nm (**b**) in 10 mM HEPES buffer solution at pH 7.1. The molar ratio of metal ion/D-P4 is 2:1. Inset in (**a**) is the color changes of the systems excited by a 365 nm UV lamp. (For interpretation of the references to color in this figure legend, the reader is referred to the Web version of this article.)

3.2. Fluorescence response of D-P4 for ions

Fig. 2 indicated the fluorescence response of D-P4 in the absence and presence of various metal ions and anions with excitation wavelength of 295 nm and 330 nm in 10 mM HEPES buffer solution (pH 7.1), respectively. The excitation wavelength at 295 nm was employed for monitoring both the Trp and dansyl fluorophore emissions, and 330 nm was employed for monitoring the dansyl fluorophore emission [43–45]. As shown in Fig. 2a, D-P4 has a maximum emission wavelength at 550 nm with excitation wavelength of 330 nm. When metal ions were added to D-P4 solution, only Hg^{2+} has a strong fluorescence enhanced response to it among these ions with a 45 nm blue shift from 550 nm to 505 nm. The increase in the fluorescence intensity with a blue shift could be attributed to a CHEF effect and a solvatochromic effect. In fact, a close packing of indole and dansyl moieties could shield at least partially the dansyl group from the solvent, thus reducing the polarity of the environment of the fluorophore [43]. This result showed that CHEF is one sensing mechanism of D-P4 to Hg^{2+}. From inset of Fig. 2a, it can be seen that D-P4 solution itself shows yellow color excited by a 365 nm UV lamp, and the addition of Hg^{2+} into D-P4 solution caused the color to green, but the D-P4 solution containing the mixed other metal ions still kept the yellow color. Fig. 2b showed that, while exciting at 295 nm, D-P4 has a fluorescence emission peak at 337 nm and 550 nm, respectively, and the addition of Hg^{2+} caused the fluorescence intensity at 337 nm decreased. When Hg^{2+} interacts with amino acid residues of D-P4, the distance of between dansyl fluorophore (acceptor) and Trp residue (donor) will shorten and it may result in the folding of D-P4, thus inducing decrease of fluorescence intensity at 337 nm and increase of fluorescence intensity at 505 nm. This result of exciting at 295 nm indicated the fluorescent resonance energy transfer (FRET) effect is another sensing mechanism of D-P4 to Hg^{2+} [43–45]. Therefore, it can be seen that the sensing mechanism of D-P4 for Hg^{2+} is by both CHEF and FRET pathways, which is consistent with that of the reported hexapeptide, dansyl-HPHGHW-NH_2 (dH3w) [43]. Compared with dH3w, both of them contain tryptophan residue (donor) and dansyl (receptor) fluorophore, but D-P4 is shorter and simpler. For different peptides which contain different amino acid residues and have different sequences, they should have different affinity for various metal ions. dH3w sensor is sensitive for Zn^{2+} and Cu^{2+}, but D-P4 is sensitive for Hg^{2+}.

Furthermore, we measured the time course for the detection of D-P4 to Hg^{2+} ion, result showed that D-P4 sensor exhibits a rapid fluorescence enhancement effect on the detection of Hg^{2+} (Fig. 3).

The energy transfer phenomenon was also confirmed through fluorescence lifetime measurements for D-P4 and D-P4-Hg (Fig. 4). When exciting at 295 nm, a decrease in the fluorescence lifetime of the donor (Trp) after binding with Hg^{2+} was observed at 337 nm emission peak, and the fluorescence lifetime was reduced from 2.80 μs to 2.77 μs. Meanwhile, when D-P4 binds to Hg^{2+}, the fluorescence lifetime of the acceptor (Dansyl) increases significantly, and the fluorescence lifetime

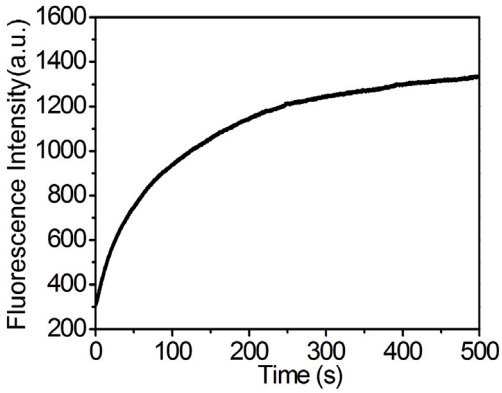

Fig. 3. Time-dependent fluorescence intensity (505 nm) change of D-P4 (20.0 μM) with the addition of Hg^{2+} (20.0 μM) in 10 mM HEPES buffer solution (pH 7.1).

increases from 7.43 μs to 11.18 μs at 505 nm emission peak, which is a typical energy resonance transfer [46].

To study the interference effect of 16 other metal ions and 9 anions on the detection ability of D-P4 for Hg^{2+}, the fluorescence responses of D-P4 to Hg^{2+} were measured in the presence of them. Fig. 5 showed the fluorescence responses of D-P4 to Hg^{2+} in the presence of other ions with excitation of 330 nm and 295 nm, respectively. Results indicated that the fluorescence response of D-P4 to Hg^{2+} was not interfered by 16 other metal ions and 9 anions.

The fluorescence spectra of D-P4 at different concentrations of Hg^{2+} in 10 mM HEPES buffer solution at pH 7.1 with excitation of 330 nm and 295 nm showed in Fig. 6. As shown in Fig. 6a, the fluorescence intensity of D-P4 at 505 nm continuously increased with the addition of Hg^{2+}. And, a 45 nm blue shift from 550 to 505 nm of the maximum fluorescence peak occurred. While exciting at 295 nm, the addition of Hg^{2+} caused the fluorescence intensity of D-P4 at 337 nm decreased, but the intensity at 505 nm increased and 45 nm blue shift occurred for this fluorescence peak (Fig. 6b).

3.3. The binding mechanism study of D-P4 with Hg^{2+}

The binding stoichiometry of D-P4 for Hg^{2+} was investigated. According to the fluorescent titration curve, about 20 μM concentration of Hg^{2+} was needed for the saturation of the fluorescence intensity of D-P4 (20.0 μM), showing that the binding ratio of D-P4 with Hg^{2+} was 1:1. Job's plot was also used to evaluate the stoichiometry of the system. The result exhibits a maximum at 0.5 mol fraction for Hg^{2+} in10 mM HEPES buffer solution at the concentration (20.0 μM) of D-P4 (Fig. 7a). This result also suggests that D-P4 formed a 1:1 complex with Hg^{2+} in HEPES buffer solution.

The binding constant of D-P4 with Hg^{2+} was obtained from the Benesi–Hildebrand equation [47,48]: $\Delta FI_{max}/\Delta FI = 1+([M]^{-n}/K)$.

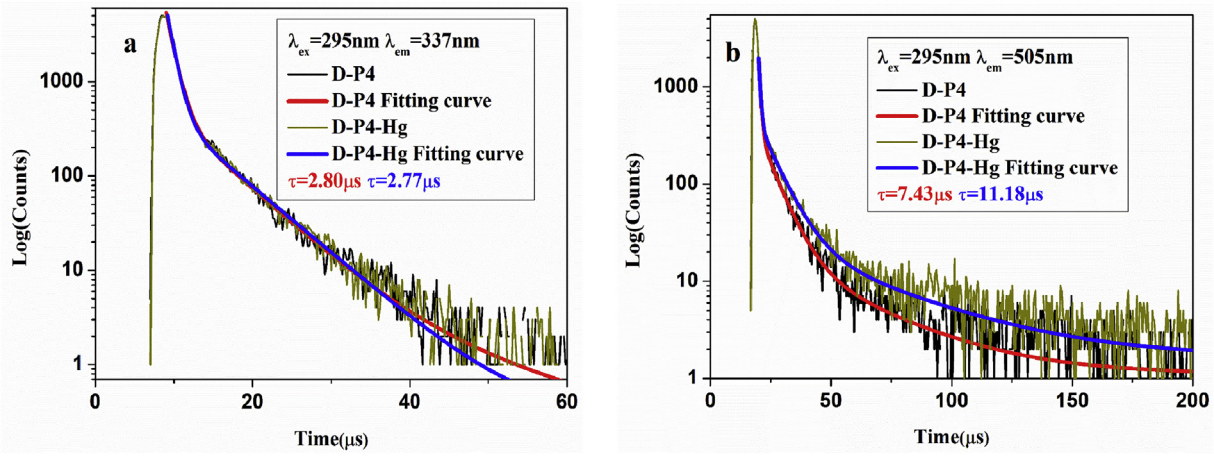

Fig. 4. Fluorescence lifetime decay profiles excited at 295 nm for D-P4 (10.0 μM) and D-P4-Hg (10.0 μM) in 10 mM HEPES buffer solution (pH 7.1) (a) λ_{max} = 337 nm, (b) λ_{max} = 505 nm.

Here, ΔFI_{max} is $FI_{max} - FI_0$, ΔFI is $F_x - F_0$; F_0 is the fluorescence intensity of D-P4 and F_x is the fluorescence intensity of D-P4 at different concentration of Hg^{2+}; [M] is the concentration of Hg^{2+} and K is the binding constant. From Fig. 7b, the binding constant of D-P4 with Hg^{2+} was estimated and the value of K was found to be $9.09 \times 10^4\ M^{-1}$.

FTIR spectrum experiment was conducted to investigate which chemical groups of D-P4 play a vital role in the interaction with Hg^{2+} (Fig. 8). The IR peaks at 3059 and 3323 cm^{-1} can be attributed to N–H and the O–H stretching vibrations in D-P4. The IR peaks at 1201 and 1668 cm^{-1} can be attributed to the C–O and C═O group. The peaks at 2363 and 2960 cm^{-1} are corresponding to stretching vibrations of O═S═O and C–H. The IR spectrum of D-P4 exhibited bands in the 1323-1525 cm^{-1} region that can be attributed to C–H deformation as well as C–N and C–S stretching vibrations. It can be observed that the stretching band of S–H at 2556 cm^{-1} is disappeared in the presence of Hg^{2+}, which suggests that the thiol group of Cys may interaction with Hg^{2+}. The observed stretching band of N–H at 3059 cm^{-1} is also disappeared in the presence of Hg^{2+}, suggesting that the amide bonds of D-P4 may be involved in the interaction of them. In addition, the changed stretching bands of C–O and C═O at 1201 and 1668 cm^{-1} in the presence of Hg^{2+} can be attributed to the binding between carboxyl groups of Glu and Hg^{2+} [49,50].

The D-P4-Hg complex was also confirmed through XPS measurement (Fig. 9). Distinct characteristic peaks corresponding to O 1s, N 1s, C 1s, Hg 4f, and S 2p were observed in both D-P4 and D-P4-Hg compounds as shown in Fig. 9a. The binding energy of S 2p for free thiol groups was between 163 and 164 eV [51]. In this study, the peak of S 2p located at 163.16 eV corresponded to the unbound thiol group as shown in Fig. 9b. In the presence of Hg^{2+}, the peak shifted from 163.16 to 162.56 eV, showing that the interaction of the thiol group (−SH) of D-P4 with Hg^{2+} resulted in the lower binding energy of S 2p. The Hg^{2+} is a soft acid and the –SH is a soft base, which can interact and form a strong coordination binding according to Hard Soft Acid Base (HSAB) principle.

1H NMR titration experiments were carried out using 50% DMSO-d_6 solution of DP-4 and tetramethylsilane as an internal standard. ^{1}H NMR (500 MHz, 50% DMSO-d_6) For Hg^{2+}:D-P4 = 0:1: *δ:* 3.06 (s, 1H), 7.861 (d, 1H), 8.243 (d, 1H); For Hg^{2+}:D-P4 = 0.5:1: *δ:* 3.06 (s, 1H), 7.884 (d, 1H), 8.240 (d, 1H); For Hg^{2+}:D-P4 = 1:1: *δ:* 3.04 (s, 1H), 7.902 (d, 1H), 8.235 (d, 1H); For Hg^{2+}:D-P4 = 2:1: *δ:* 2.91 (s, 1H), 8.086 (d, 1H), 8.158 (d, 1H). As seen from Fig. 10, with the incremental amounts of Hg^{2+} to DP-4, the H peaks of DP-4 gradually changed and then unchanged after the addition of 1 equivalent of Hg^{2+}. This result clearly indicated that Hg^{2+} coordinated with the specific functional groups of DP-4 and their binding ratio is 1:1.

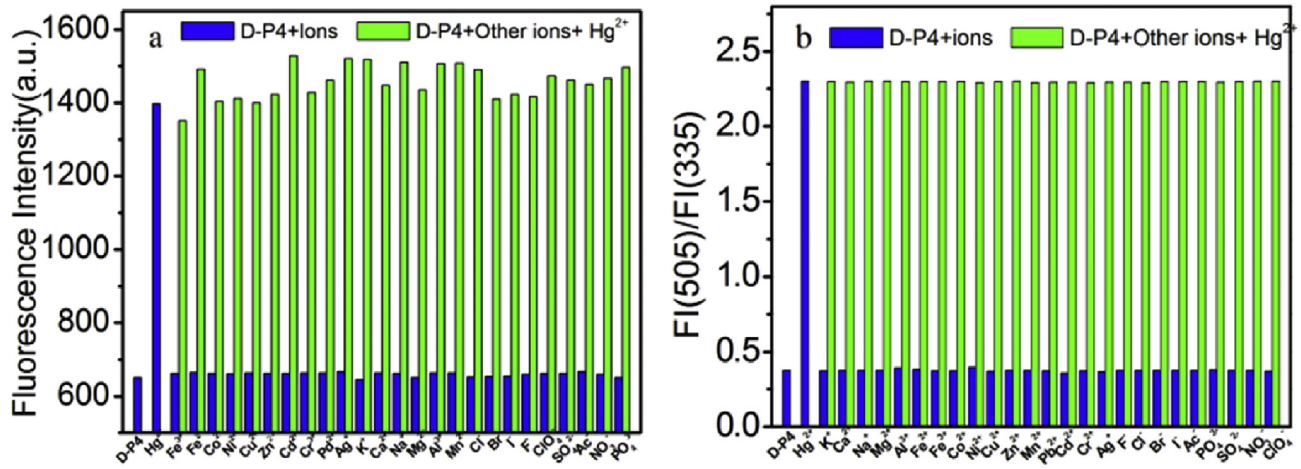

Fig. 5. Fluorescence response of D-P4 (20.0 μM) to Hg^{2+} in the presence of 16 metal ions and 9 anions (1 equiv.) with excitation wavelength of 330 nm (**a**) and 295 nm (**b**) in 10 mM HEPES solution at pH 7.1. The blue bars represent the addition of these ions (20 μM) to D-P4 solution. The green bars represent the subsequent addition of 20 μM Hg^{2+} to the above solutions. (For interpretation of the references to color in this figure legend, the reader is referred to the Web version of this article.)

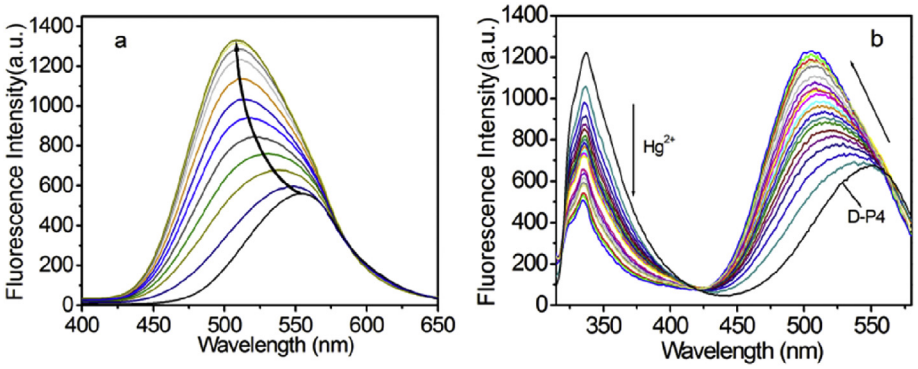

Fig. 6. Fluorescence spectra of D-P4 (20.0 μM) with excitation wavelength of 330 nm (**a**) and 295 nm (**b**) upon addition of increasing concentrations of Hg^{2+} (0–22 μM) in 10 mM HEPES buffer at pH 7.1.

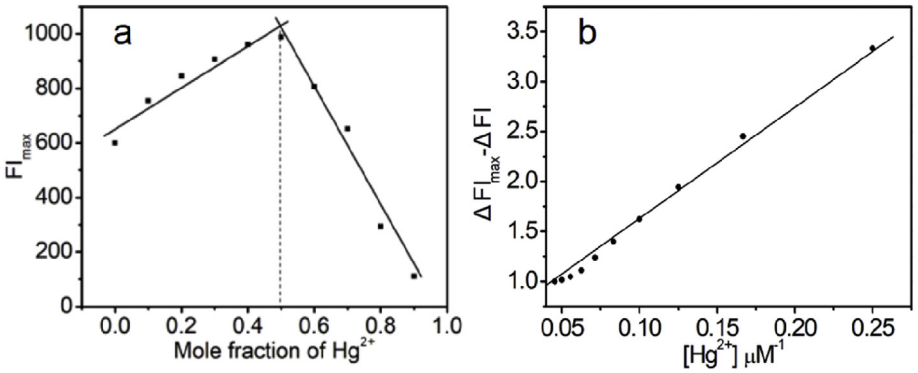

Fig. 7. a.Job's plot for D-P4 with Hg^{2+} in 10 mM HEPES buffer solution at pH 7.1. Fig. 7b Benesi-Hildebrand plot for the determination of the binding constant of D-P4 (20.0 μM) with Hg^{2+}.

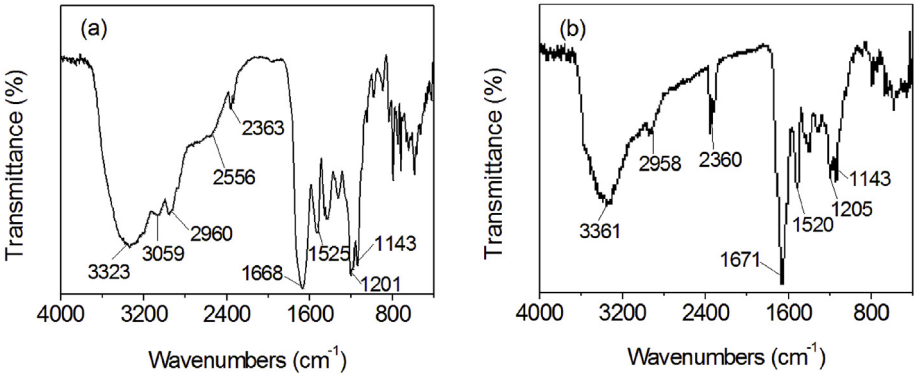

Fig. 8. IR spectra of D-P4 and D-P4-Hg complex.

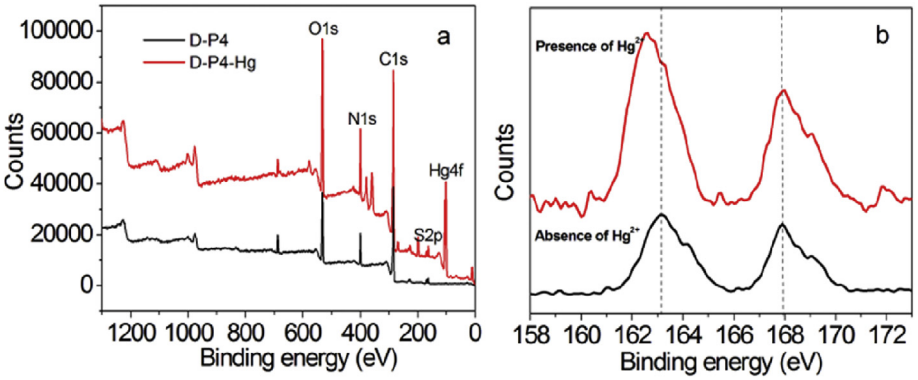

Fig. 9. XPS spectra of D-P4 and D-P4-Hg complex.

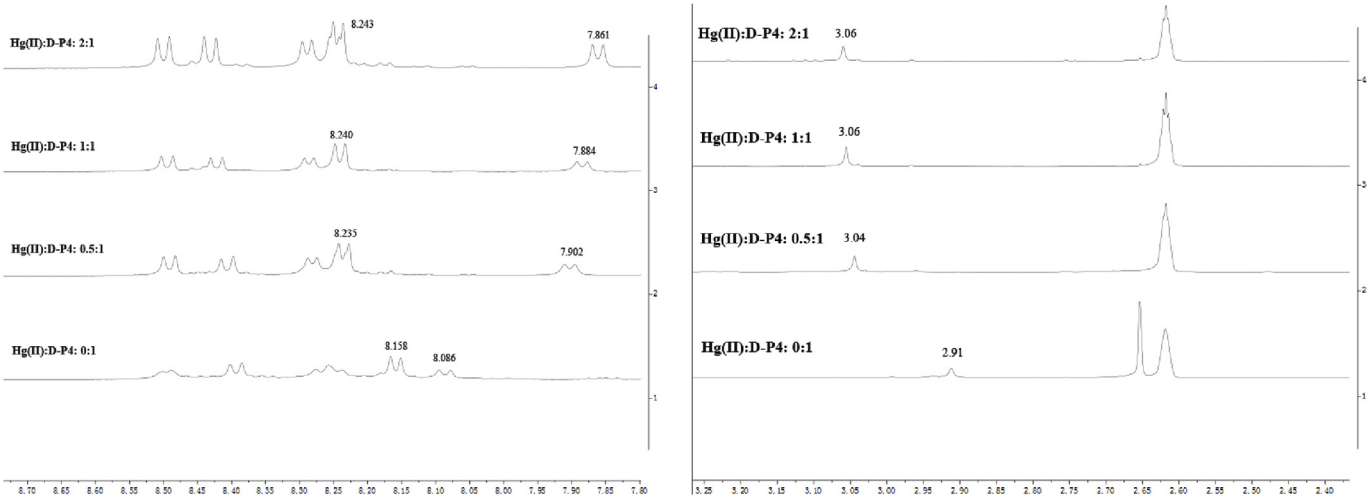

Fig. 10. ^{1}H NMR titration spectra of D-P4 in the absence and presence of Hg^{2+}.

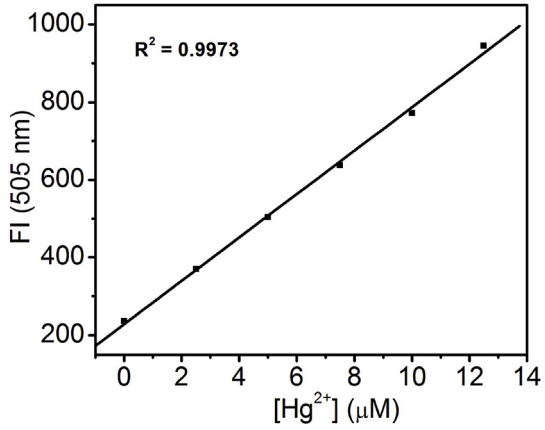

Fig. 11. Linear relationship of fluorescence intensity at 505 nm with the concentration of Hg^{2+} in 10 mM HEPES buffer solution at pH 7.1.

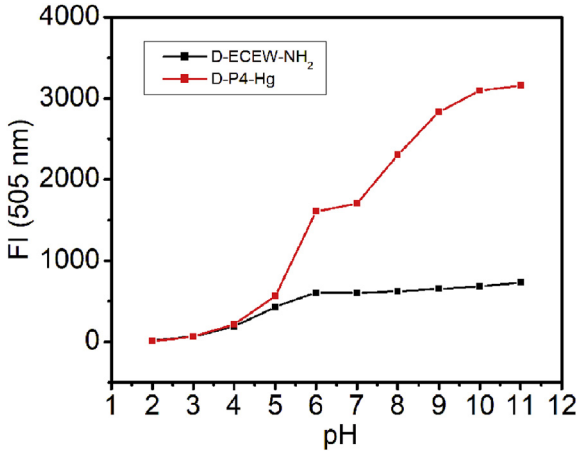

Fig. 12. Fluorescence intensity of D-P4 (20.0 μM) in the absence and presence of Hg^{2+} (1 equiv.) at different pH values.

3.4. Detection limit of D-P4 for Hg^{2+}

The limit of detection (LOD) was calculated by the fluorescence titration experiments. In order to ascertain the S/N ratio, the fluorescence intensity of D-P4 in the absence of Hg^{2+} ion was measured ten times and the standard deviation of blank measurement was obtained.

Table 2
Determination of Hg^{2+} in river water.

Sample	Added Hg^{2+} (μM)	Detected Hg^{2+} (μM)	Recovery ratio (%)
1	0.1	0.106	106
2	0.3	0.29	96.7
3	0.6	0.57	95
4	1	1.03	103
5	1.5	1.52	101

Three independent duplication measurements of fluorescence intensity were evaluated in the presence of Hg^{2+} ion and the mean intensity was plotted as a function of Hg^{2+} concentration for determining the slope. Then, the LOD for Hg^{2+} was obtained by the equation: LOD = 3σ/m, where σ is the standard deviation of the fluorescence intensity of D-P4, m is the slope of the curve of the plot [52]. Fig. 11 showed a good linear relationship between the fluorescence intensity and Hg^{2+} concentration in the range of 0–14 μM with correlation cofficient R^2 = 0.9973. According to the equation LOD = 3σ/m, the detection limit of D-P4 for Hg^{2+} is 23.0 nM.

3.5. Effects of pH on the detection

The influence of pH on the fluorescence detection of D-P4 for Hg^{2+} was measured, as shown in Fig. 12. Results indicate that D-P4 and D-P4-Hg showed a weak fluorescence intensity in acidic solution (pH < 5), which because that the charge transfer between dimethylamino group and naphthyl moiety was prevented by the protonated dimethylamino group of fluorophore dansyl chloride [53,54]. When pH 8–11, the negative charge for the sulfhydryl group of cysteine and the free carboxyl group of glutamic acid in D-P4 is increasing, which can enhance formation of the D-P4-Hg complex, thus resulting the fluorescence intensity of D-P4-Hg system increased. Overall results indicated that D-P4 was a useful analytical tool for monitoring Hg^{2+} at neutral or alkaline environment.

3.6. Application of D-P4 for detecting Hg^{2+}

In order to test the practical application of D-P4 for detecting Hg^{2+}, the standard detection curve of Hg^{2+} was obtained by standard addition of Hg^{2+} ion to D-P4 (20 μM) solution. In the same way, the same concentration of Hg^{2+} ion was added to the river water solution containing D-P4 to obtain the measurement curve. By comparing the calculated ion concentration with the actual concentration, the accuracy and practicability of the detection method can be judged. Results were

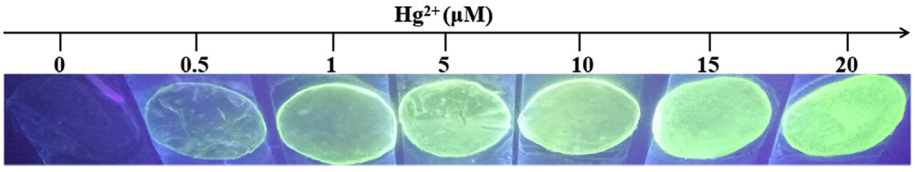

Fig. 13. Visual detection of Hg^{2+} using D-P4 agarose gel flake under a 365 nm UV lamp.

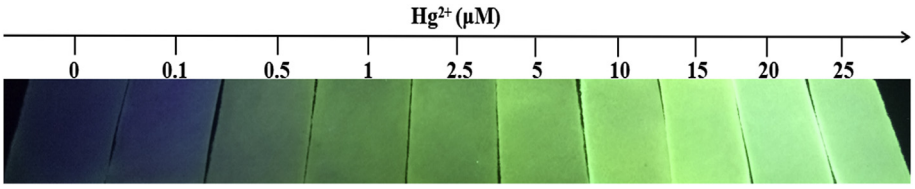

Fig. 14. Visual detection of Hg^{2+} using D-P4 test paper under a 365 nm UV lamp.

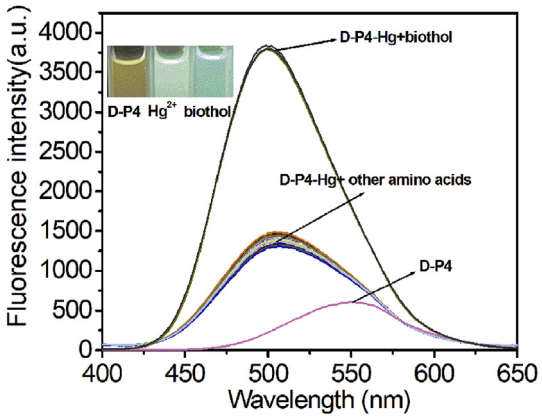

Fig. 15. Fluorescence spectra of D-P4-Hg (20.0 μM) excitated at 330 nm in the absence and presence of biothiols (Cys, Hcy and GSH) and other 19 amino acids (20.0 μM) in 10 mM HEPES buffer at pH 7.1. Inset: Emission color changes of D-P4, D-P4-Hg and D-P4-Hg-biothiols systems excited by a 365 nm UV lamp. (For interpretation of the references to color in this figure legend, the reader is referred to the Web version of this article.)

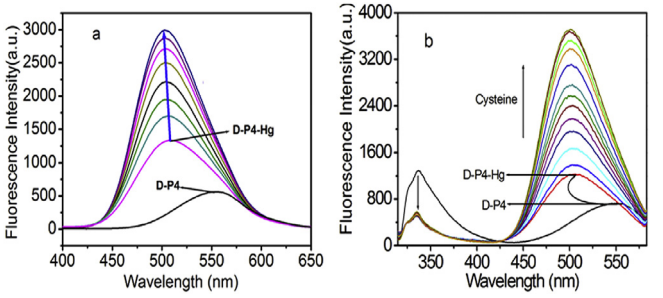

Fig. 16. Fluorescence spectra of D-P4-Hg (20.0 μM) with addition of increasing concentrations of Cys (0–20.0 μM) in pH 7.1, 10 mM HEPES buffer at λ_{ex} = 330 nm (**a**) and λ_{ex} = 295 nm (**b**).

summarized in Table 2, it showed that this peptide based sensor exhibits a good recovery for Hg^{2+} in the range from 0.1 to 1.5 μM for monitoring Hg^{2+} ion in river water. Therefore, the results indicated that D-P4 can be used to monitor Hg^{2+} ion in river water and has potential applications in environment.

In order to achieve effective visual detection of Hg^{2+}, D-P4 is dissolved in agarose solution to make a circular gel sheet. D-P4 agarose gel flakes were placed in the aqueous solution containing different concentration of Hg^{2+} and placed for 10 min. The color of the prepared gel flakes observed under the 365 nm UV lamp is shown in Fig. 13. The fluorescent green color gradually deepened with the increment of Hg^{2+} concentration from 0 to 20 μM. In addition, D-P4 test papers were

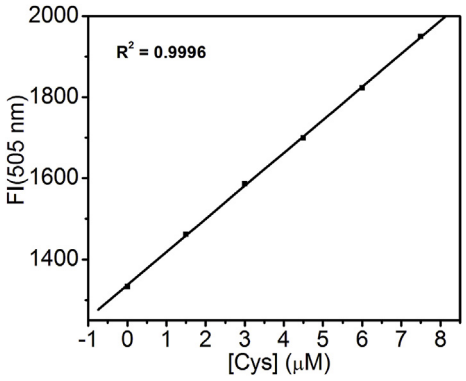

Fig. 17. Linear relationship of fluorescence intensity at 505 nm with concentration of Cys.

Table 3
Various spectral sensing systems for determination of Cys.

Method	System	LOD	Reference
Fluorescence	"T-Hg^{2+}-T" system	2.4 nM	51
Fluorescence	Sensor based on fluorescein and triethylamine	0.5 μM	52
Fluorescence	Naphthofluorescein-based near-infrared (NIR)	0.18 μM	53
Fluorescence	Coumarin-based compound	0.463 μM	54
Fluorescence	4,5-di((E)-styryl)-1H-imidazole dye and aldehyde group	0.18 μM	55
Fluorescence	π-conjugated triarylboron luminogen	0.18 μM	56
Fluorescence	Curcumin and Hg^{2+} system	1.0 μM	57
Fluorescence	NBD	98 nM	58
Absorption	PBI- Hg^{2+}	91.0 nM	59
Fluorescence	Naphthol AS-based sensor	0.5 μM	60
Fluorescence	A benzothiazole derivative	84 nM	61
Fluorescence	Crotonoyl ester-functionalized oxazolidinoindole	5.0 μM	62
Fluorescence	Diketopyrrolopyrrole-based chemodosimeter	5.0 μM	63
Absorption	L-Hg^{2+} complex	0.1 μM	64
Absorption	DNA-Gold Nanoparticle	100 nM	65
Fluorescence	Rhodol	0.6 μM	66
Fluorescence	Acridine orange	110 nM	67
Fluorescence	A rhodol thioester	44 nM	68
Fluorescence	Pyrenedione	0.15 μM	69
Fluorescence	Quinazoline platform	0.35 μM	70
Fluorescence	D-P4-Hg system	52.0 nM	This work

prepared by immersing the dried filter paper in 20 μM D-P4 solution. On Immersing the test paper in the aqueous solution of different concentration of Hg^{2+}, the colors of the test papers from colorless to green with the increment of Hg^{2+} concentration from 0 to 25 μM under 365 nm UV lamp, as shown in Fig. 14. Results suggest that D-P4 agarose

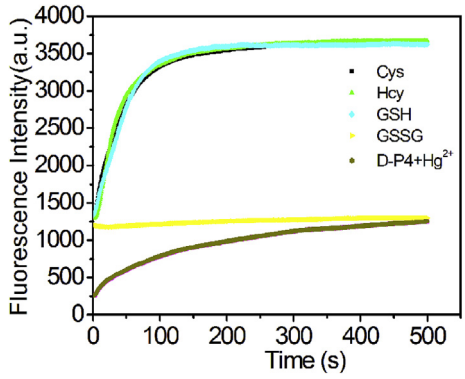

Fig. 18. Time-dependent fluorescence intensity (505 nm) change of D-P4-Hg (20.0 μM) with the addition of biothiols (20.0 μM) in 10 mM HEPES buffer solution (pH 7.1).

gel flake and D-P4 test paper can be used to the visual detection of Hg^{2+} in water samples.

3.7. Fluorescence response of D-P4-Hg to biothiols

It is very interesting and noteworthy that the D-P4-Hg systems can be used to detect biothiols (Cys, Hcy and GSH). The fluorescence spectrum of D-P4 sensor was not affected by these biothiols itself. However, when these biothiols were added to D-P4-Hg system solution, the fluorescence intensity of D-P4-Hg systems were strongly enhanced (Fig. 15). And, other 19 amino acids were not affected the spectra of D-P4-Hg system, inferring that D-P4-Hg system can be selective response to biothiols.

Fig. 16 is fluorescence spectra of D-P4-Hg system at different concentrations of Cys (0–20.0 μM) in 10 mM HEPES buffer at pH 7.1. From Fig. 16, it can be seen that the fluorescence intensity excitated at 330 nm gradually enhanced when the increasing concentrations of Cys were added to the D-P4-Hg solutions (Fig. 16a). From Fig. 16b, with excitation of 295 nm, the fluorescence intensity at 505 nm wavelength was enhanced with the addition of Cys, but the fluorescence intensity at 337 nm wavelength was not change. Results indicated that the addition of Cys can not chance the FRET effect between dansyl fluorophore and Trp residue, but it can enhance the CHEF effect. It may be that Cys occupied a week mercury ion coordination site on D-P4 to form a new ternary complex, inducing the CHEF effect of dansyl fluorophore.

Some paper reported on the use of Hg^{2+}-sensor complex to indirectly detect Cys mainly by using the thiol group on Cys to bind the Hg^{2+} on Hg^{2+}-sensor complex, thereby recovering its spectral peak [55–57]. While in this study, for this D-P4-Hg system which itself contains thiol group, the addition of Cys does not capture Hg^{2+} from D-P4-Hg system, but forms a ternary complex with them, changing the microenvironment of dansyl fluorophore to induce CHEF effect, resulting in a sharp increase in the intensity of the fluorescent peak.

The fluorescence intensity changes present a good linear relationship to Cys at low concentration for D-P4-Hg system with correlation coefficient $R^2 = 0.9996$. Based on this analysis method, the limit of detection for Cys was 52.0 nM (Fig. 17). From Table 3, it can be seen that the D-P4-Hg system has lower detection limit for Cys than that in previous reports [55–74]. Furthermore, fluorescence kinetics experiment showed that the D-P4-Hg system exhibits a rapid fluorescence enhancement effect on the detection of biothiols (Cys, Hcy and GSH) (Fig. 18).

Table 4
Determination of total thiols in human serum samples using D-P4-Hg system.

Serum samples	Content of serum	Determined biothiols (μM)	Added Cysteine (μM)	Measured (μM)	Recovery (%)
1	10%	49.8	100.0	146.2	97.6
2	30%	151.6	100.0	272.0	108.1
3	50%	257.2	100.0	378.6	106.0
4	70%	348.6	100.0	441.4	98.4

3.8. Visible detection for Hg^{2+} and biothiols

Fig. 19a is the visible emission color changes of D-P4 solution in the absence and presence of Hg^{2+} and other ions excited by a 365 nm UV lamp. D-P4 solution itself showed yellow color, the addition of Hg^{2+} into D-P4 solution caused the color from yellow to green, and the D-P4 solutions containing other ions kept the yellow color. Fig. 19b showed that the green color of D-P4-Hg system solutions grow rapidly lighter upon the addition of biothiols (GSH, Hcy and Cys), and remained unchanged when exposed to 19 other amino acids under a 365 nm UV lamp. This phenomenon of color change of this chemosensor could be used to determine Hg^{2+} and biothiols.

3.9. Application of D-P4-Hg for detecting biothiol

Yin et al. have reported some novel fluorescent sensor for biothiols detection and its application [75–78]. In order to evaluate the applicability of D-P4-Hg system for the determination of biothiols in biological samples. Human serum samples were diluted to 10%, 30%, 50% and 70% with 10 mM phosphate-buffered saline(pH 7.1) before determination. We measured the total biothiol content in this human serum sample was 510 μM, in agreement with the concentration of the total biothiol in human blood [79]. The total biothiol content of human serum was concluded by the standard titration experiment of cysteine and the results are shown in Table 4. The recovery results ranged from 97.6% to 108.1%, suggesting that no significant interference with the determination of biothiols in serum samples was encountered after an

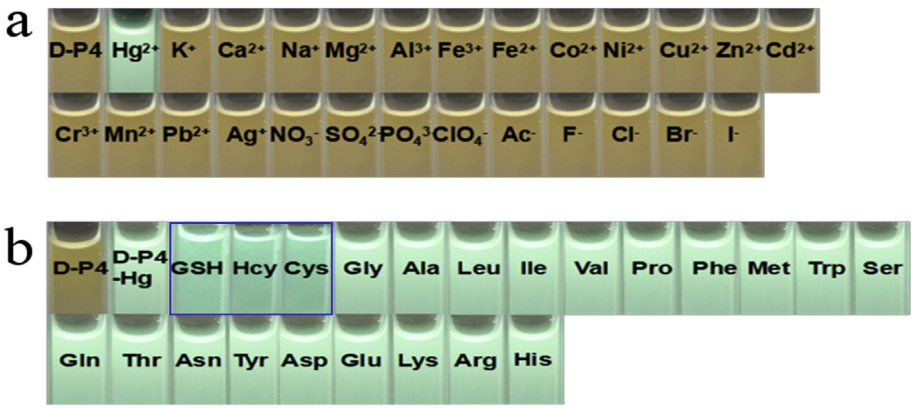

Fig. 19. a.Emission color changes of D-P4 (20 μM) upon addition of 1 equiv of 17 metal ions and 9 anions in 10 mM HEPES buffer solution at pH 7.1; Fig. 19b Emission color changes of D-P4-Hg (20 μM) system upon addition of 1 equiv of GSH, Hcy, Cys and other 19 amino acids in 10 mM HEPES buffer solution at pH 7.1. (For interpretation of the references to color in this figure legend, the reader is referred to the Web version of this article.)

appropriate dilution of the samples. It was found that D-P4-Hg system great potential for detecting biothiols in biological samples.

4. Conclusions

In conclusion, we have developed a simple peptidyl dual-functional fluorescent chemosensor (D-P4) for Hg^{2+} and biothiols. This chemosensor showed turn on response to Hg^{2+} with a low limit of detection based on FRET effect and CHEF effect, which was not interfered by the tested metal ions in HEPES buffer solution. Furthermore, we have successfully detected biothiols including GSH, Hcy and Cys by using the D-P4-Hg system. Thus, these results suggested that the peptidyl fluorescent chemosensor can be capable of performing multifunctional monitor via different mechanisms in environmental systems. We hope this study can promote the further development of multifunctional probe based on peptide by optimizing modifiable amino acid sequence for lots of practical applications in environmental and biological systems.

Acknowledgements

This work was supported by the Scientific Research Foundation of Liaocheng University, China (2019, 318011513), and the National Natural Science Foundation of China (21142003, 20471025).

Appendix A. Supplementary data

Supplementary data to this article can be found online at https://doi.org/10.1016/j.dyepig.2019.107888.

References

[1] Duong TQ, Kim JS. Fluoro- and chromogenic chemodosimeters for heavy metal ion detection in solution and biospecimens. Chem Rev 2010;110:6280–301.
[2] Saidur MR, Aziz AR, Basirun WJ. Recent advances in DNA-based electrochemical biosensors for heavy metal ion detection: a review. Biosens Bioelectron 2017;90:125–39.
[3] Nolan EM, Lippard SJ. Tools and tactics for the optical detection of mercuric ion. Chem Rev 2008;108:3443–80.
[4] Zhou N, Chen H, Li J, Chen L. Highly sensitive and selective voltammetric detection of mercury(II) using an ITO electrode modified with 5-methyl-2-thiouracil, graphene oxide and gold nanoparticles. Microchim Acta 2013;180:493–9.
[5] Sivaraman G, Anand T, Chellappa D. Development of a pyrene based "turn on" fluorescent chemosensor for Hg^{2+}. RSC Adv 2012;2:10605–9.
[6] Lisha KP, Anshup Pradeep T. Towards a practical solution for removing inorganic mercury from drinking water using gold nanoparticles. Gold Bull 2009;42:144–52.
[7] Jeong Y, Yoon J. Recent progress on fluorescent chemosensors for metal ions. Inorg Chim Acta 2012;381:2–14.
[8] Li G, Tao F, Liu Q, Wang L, Wei Z, Zhu F, Chen W, Sun H, Zhou Y. A Highly selective and reversible watersoluble- polymer based colorimetric chemosensor for rapid detection of Cu^{2+} in pure aqueous solution. New J Chem 2016;40. 4513-4518.
[9] Yue Q, Shen T, Wang J, Wang L, Xu S, Li H, Liu J. A reusable biosensor for detecting mercury(II) at the subpicomolar level based on “turn-on” resonance light scattering. Chem Commun 2013;49:1750–2.
[10] Shen T, Yue Q, Jiang X, Wang L, Xu S, Li H, Gu X, Zhang S, Liu J. A reusable and sensitive biosensor for total mercury in canned fish based on fluorescence Polarization. Talanta 2013;117:81–6.
[11] Wang LJ, Jia LP, Ma RN, Jia WL, Wang HS. A colorimetric assay for Hg^{2+} detection based on Hg^{2+}-induced hybridization chain reactions. Anal Methods 2017;9:5121–6.
[12] Zhang Y, Li R, Xue Q, Li H, Liu J. Colorimetric determination of copper(II) using a polyamine-functionalized gold nanoparticle probe. Microchim Acta 2015;182:1677–83.
[13] Su Q, Niu Q, Sun T, Li T. A simple fluorescence turn-on chemosensor based on Schiff-base for Hg^{2+} selective detection. Tetrahedron Lett 2016;57:4297–301.
[14] Zhong Z, Zhang D, Li D, Zheng Z, Tian Z. Turn-on fluorescence sensor based on naphthalene anhydride for Hg^{2+}. Tetrahedron 2016;72:8050–4.
[15] White BR, Liljestrand HM, Holcombe JA. A 'turn-on' FRET peptide sensor based on the mercury binding protein MerP. Analyst 2008;133:65–70.
[16] Malkondu S, Erdemir S. A novel perylene-bisimide dye as “turn on” fluorescent sensor for Hg^{2+} ion found in DMF/H_2O. Dyes Pigments 2015;113:763–9.
[17] Kim SH, Kim JS, Mi Park S, Chang SK. Hg^{2+}-selective off − on and Cu^{2+} selective on − off type fluoroionophore based upon cyclam. Org Lett 2006;8:371–4.
[18] Lee S, Rao BA, Son YA. A highly selective fluorescent chemosensor for Hg^{2+}, based on a squaraine–bis(rhodamine-B) derivative: Part II. Sens Actuators B Chem 2015;210:519–32.
[19] Wanichacheva N, Setthakarn K, Prapawattanapol N, Hanmeng O, Lee VS, Grudpan K. Rhodamine B-based “turn-on” fluorescent and colorimetric chemosensors for highly sensitive and selective detection of mercury (II) ions. J Lumin 2012;132:35–40.
[20] Wanichacheva N, Hanmeng O, Kraithong S, Sukrat K. Dual optical Hg^{2+} selective sensing through FRET system of fluorescein and rhodamine B fluorophores. J Photochem Photobio A Chem 2014;278:75–81.
[21] Chen J, Li Y, Zhong W, Wang H, Zhang P, Jiang J. A highly selective fluorescent and colorimetric chemosensor for Hg^{2+} based on a new rhodamine derivative. Anal Methods 2016;8:1964–7.
[22] Park J, In B, Lee KH. Highly selective colorimetric and fluorescent detection for Hg^{2+} in aqueous solutions using a dipeptide-based chemosensor. RSC Adv 2015;5:56356–61.
[23] Wu FY, Zhao YQ, Ji ZJ, Wu YM. A highly sensitive and selective fluorescent chemodosimeter for Hg^{2+} in neutral aqueous solution. J Lumin 2007;17:460–5.
[24] Joshi BP, Park J, Lee WI, Lee KH. Ratiometric and turn-on monitoring for heavy and transition metal ions in aqueous solution with a fluorescent peptide sensor. Talanta 2009;78:903–9.
[25] Kim DH, Seong J, Lee H, Lee KH. Ratiometric fluorescence detection of Hg(II) in aqueous solutions at physiological pH and live cells with a chemosensor based on tyrosine. Sens Actuators B Chem 2014;196:421–8.
[26] Song H, Liu Q, Li Y, Wei F, Cai S, Lu Y, Zeng X. Rhodamine 6G-based chemosensor for the visual detection of Cu^{2+}, and fluorescent detection of Hg^{2+}, in water. Chem Res Chin Univ 2014;30:32–6.
[27] Wang J, Wang Y, Dong Y, Lu L, Li Q, Wang Z, Zhang Y. Modified capillary electrophoresis for highly sensitive and selective detection of Hg^{2+} in natural water. J Chin Chem Soc-Taip 2016;63:417–23.
[28] Wang P, Liu L, Zhou P, Wu W, Wu J, Liu W, Tang Y. A peptide-based fluorescent chemosensor for multianalyte detection. Biosens Bioelectron 2015;72:80–6.
[29] Adhikari S, Ghosh A, Ghosh M, Guira S, Das D. Ratiometric sensing of Fe^{3+}, through PET-CHEF-FRET processes: live cell imaging, speciation and DFT studies. Sens Actuators B Chem 2017;251:942–50.
[30] Gao M, Xie P, Wang L, Miao X, Guo F. A new optical sensor for Al^{3+}/Fe^{3+}, based on PET and chelation-enhanced fluorescence. Res Chem Intermed 2015;41:9673–85.
[31] Liu Q, Wang J, Boyd BJ. Peptide-based biosensors. Talanta 2015;136:114–27.
[32] White BR, Liljestrand HM, Holcombe JA. A 'turn-on' FRET peptide sensor based on the mercury binding protein MerP. Analyst 2007;133:65–70.
[33] Choulier L, Shvadchak VV, Naidoo A, Klymchenko AS, Mély Y, Altschuh D. A peptide-based fluorescent ratiometric sensor for quantitative detection of proteins. Anal Biochem 2010;401:188–95.
[34] Gerasimov JY, Lai RY. Design and characterization of an electrochemical peptide-based sensor fabricated via "click" chemistry. Chem Commun 2011;47:8688–90.
[35] Pang X, Gao L, Feng H, Li X, Kong J, Li Li. A peptide-based multifunctional fluorescent probe for Cu^{2+}, Hg^{2+} and biothiol. New J Chem 2018;42:15770–7.
[36] Feng H, Gao L, Ye X, Wang L, Xue Z, Kong J, Li L. Synthesis of a heptapeptide and its application in the detection of mercury(II) ion. Chem Res Chin Univ 2017;33:155–9.
[37] Wang Z, Feng H, Li Y, Xu T, Xue Z, Li L. A high selective fluorescent ratio sensor for Cd^{2+} based on the interaction of peptide with metal ion, Chin. J Inorg Chem 2015;31:1946–52.
[38] Wang L, Tian Y, He X, Zhao B, Ma W, Yang J, Song B. A new “on-off-on” fluorescent sensor for cascade recognition of Hg^{2+} and S^{2-} ion in aqueous medium. J Photochem Photobiol, A 2018;358:300–6.
[39] Qu W, Yang L, Hang Y, Zhang X, Qu Y, Hua J. Photostable red turn-on fluorescent diketopyrrolopyrrole chemodosimeters for the detection of cysteine in living cells. Sens Actuators B Chem 2015;211:275–82.
[40] Tang Y, Jin L, Yin B. A dual-selective fluorescent probe for GSH and Cys detection: emission and pH dependent selectivity. Anal Chim Acta 2017;993:87–95.
[41] Ramar R, Malaichamy I. Naked eye and optical biosensing of cysteine over the other amino acids using β-cyclodextrin decorated silver nanoparticles as a nanoprobe. New J Chem 2018;42:9193–9.
[42] Hooshmand B, Polvikoski T, Kivipelto M, Tanskanen M, Myllykangas L, Erkinjuntti T, Mäkelä M, Oinas M, Paetau A, Scheltens P, van Straaten EC, Sulkava R, Solomonet A. Plasma homocysteine, Alzheimer and cerebrovascular pathology: a population-based autopsy study. Brain 2013;136:2707–16.
[43] Donadio G, M Di artino R, Oliva R, Petraccone L, Del Vecchio P, Di Luccia B, Ricca E, Isticato R, Di Donato A, Notomista E. A new peptide-based fluorescent probe selective for zinc(II) and copper(II). J Mater Chem B 2016;4:6979–88.
[44] Wang P, Wu J, Zhou P, Liu W, Tang Y. A novel peptide-based fluorescent chemosensor for measuring zinc ions using different excitation wavelengths and application in live cell imaging. J Mater Chem B 2015;3:3617–24.
[45] Li Y, Li L, Pu X, Ma G, Wang E, Kong J, Liu Z, Liu Y. Synthesis of a ratiometric fluorescent peptide sensor for the highly selective detection of Cd^{2+}. Bioorg Med Chem Lett 2012;22:4014–7.
[46] Nowacka M, Kowalewska A, Plażuk D, Makowski T. Hybrid polysilsesquioxanes for fluorescence resonance energy transfer. Dyes Pigments 2019;170:107622.
[47] Sarkar S, Roy S, Saha RN, Panja SS. Thiophene appended dual fluorescent sensor for detection of Hg^{2+} and cysteamine. J Fluoresc 2018;1:1–11.
[48] Das S, Sahana A, Banerjee A, Lohar S, Safin DA, Babashkina MG, Bolte M, Garcia Y, Hauli I, Mukhopadhyay SK, Das D. Ratiometric fluorescence sensing and intracellular imaging of Al^{3+} ions driven by an intramolecular excimer formation of a pyrimidine-pyrene scaffold. Dalton Trans 2013;14:4757–63.
[49] Sun X, Yang S, Guo M, Ma S, Zheng M, He J. Reversible fluorescence probe based on N-doped carbon dots for the determination of mercury ion and glutathione in waters and living cells. Anal Sci 2017;33:761–7.
[50] Jun KH, Oh S, Park J, Park YJ, Park SH, Lee KH. A novel fluorescent peptidyl probe

for highly sensitive and selective ratiometric detection of Cd(II) in aqueous and biosamples via metal ion-mediated self-assembly. New J Chem 2018;42:18143–51.
[51] Bhatt R, Kushwaha S, Bojja S, Padmaja P. Chitosan-thiobarbituric acid: a super-adsorbent for mercury. ACS Omega 2018;3:13183–94.
[52] Neupane LN, Kim JM, Lohani CR, Lee KH. Selective and sensitive ratiometric detection of Hg^{2+} in 100% aqueous solution with triazole-based dansyl probe. J Mater Chem 2012;22:4003–8.
[53] Métivier R, Leray I, Valeur B. Lead and mercury sensing by calixarene-based fluoroionophores bearing two or four dansyl fluorophores. Chem Eur J 2004;10:4480–90.
[54] O'Connor NA, Sakata ST, Zhu H, Shea KJ. A fluorescent diagnostic for ion and proton detection in solution and in polymers. Org Lett 2006;8:1581–4.
[55] Chen X, Liu H, Wang C, Hu H, Wang Y, Zhou X, Hu J. A label-free fluorescence turn-on sensor for rapid detection of cysteine. Talanta 2015;138:144–8.
[56] Geng F, Wang Y, Qu P, Zhang Y, Dong H. Naked-eye detection of Cys using simple molecular systems of curcumin and Hg^{2+}. Anal Methods 2013;5:3965–9.
[57] Jung JM, Kim C, Harrison RG. A dual sensor selective for $Hg2^{+}$ and cysteine detection. Sens Actuators B Chem 2018;255:2756–63.
[58] Wang L, Zhou Q, Zhu B, Yan L, Ma Z, Du B, Zhang X. A colorimetric and fluorescent chemodosimeter for discriminative and simultaneous quantification of cysteine and homocysteine. Dyes Pigments 2012;95:275–9.
[59] Xue S, Ding S, Zhai Q, Zhang H, Feng G. A readily available colorimetric and near-infrared fluorescent turn-on probe for rapid and selective detection of cysteine in living cells. Biosens Bioelectron 2015;68:316–21.
[60] Yang Y, Wang H, Wei YL, Zhou J, Zhang JF, Zhou Y. A selective coumarin-based "turn-on" fluorescent sensor for the detection of cysteine and its applications for bioimaging. Chin Chem Lett 2017;28:2023–6.
[61] Shen Y, Zhang X, Zhang Y, Zhang C, Jin J, Li H, Yao H. A novel colorimetric/fluorescence dual-channel sensor based on NBD for the rapid and highly sensitive detection of cysteine and homocysteine in living cells. Anal Methods 2016;8:2420–6.
[62] Fang HP, Shellaiah M, Singh A, Raju MVR, Wu YH, Lin HC. Naked eye and fluorescent detections of Hg^{2+}, ions and Cysteine via J-aggregation and deaggregation of a perylene bisimide derivative. Sens Actuators B Chem 2014;194:229–37.
[63] Long L, Wang L, Wu Y. A fluorescence ratiometric probe for cysteine/homocysteine and its application for living cell imaging. Int J Org Chem 2013;03:235–9.
[64] Ma WW, Wang MY, Yin D, Zhang X. Facile preparation of naphthol AS-based fluorescent probe for highly selective detection of cysteine in aqueous solution and its imaging application in living cells. Sens Actuators B Chem 2017;248:332–7.
[65] Feng S, Li X, Ma Q, Liang B, Ma Z. A highly selective and sensitive fluorescent probe for thiols based on a benzothiazole derivative. Anal Methods 2016;8:6832–9.
[66] Kim CY, Kang HJ, Chung SJ, Kim HK, Na SY, Kim HJ. Mitochondria-targeting chromogenic and fluorescence turn on probe for the selective detection of cysteine by caged oxazolidinoindocyanine. Anal Chem 2016;88:7178–82.
[67] Yang L, Li X, Qu Y, Qu W, Zhang X, Hang Y, Agren H, Hua J. Red turn-on fluorescent phenazine-cyanine chemodosimeters for cyanide anion in aqueous solution and its application for cell imaging. Sens Actuators B Chem 2014;203:833–47.
[68] Lee JS, Ulmann PA, Han MS, Mirkin CA. A DNA-gold nanoparticle-based colorimetric competition assay for the detection of cysteine. Nano Lett 2008;8:529–33.
[69] Liu Y, Xiang K, Tian B, Zhang J. Rhodol-based far-red fluorescent probe for the detection of cysteine and homocysteine over glutathione. Luminescence 2017;32:78–85.
[70] Guo X, Zhang X, Wang S, Li S, Hu R, Li Y. Sensing for intracellular thiols by water-insoluble two-photon fluorescent probe incorporating nanogel. Anal Chim Acta 2015;869:81–8.
[71] Tang Y, Jin L, Yin B. A dual-selective fluorescent probe for GSH and Cys detection: emission and pH dependent selectivity. Anal Chim Acta 2017;993:87–95.
[72] Yang XF, Huang Q, Zhong Y, Li Z, Li H, Lowry M, Escobedo JO, Strongin RM. A dual emission fluorescent probe enables simultaneous detection of glutathione and cysteine/homocysteine. Chem Sci 2014;5:2177–83.
[73] Zhang Y, Yao W, Liang D, Sun M, Wang S, Huang D. Selective detection and quantification of tryptophan and cysteine with pyrenedione as a turn-on fluorescent probe. Sens Actuators B Chem 2018;259:768–74.
[74] Anand T, Sivaraman G, Chellappa D. Hg^{2+} mediated quinazoline ensemble for highly selective recognition of Cysteine. Spectrochim Acta 2014;123:18–24.
[75] Xie X, Yin C, Yue Y, Huo F. Rational design of fluorescent probe for Cys dynamics imaging in living cell. Sens Actuators B Chem 2018;267:76–82.
[76] Li X, Huo F, Yue Y, Zhang Y, Yin C. A coumarin-based "off-on" sensor for fluorescence selectivily discriminating GSH from Cys/Hcy and its bioimaging in living cells. Sens Actuators B Chem 2017;253:42–9.
[77] Yin C, Zhang W, Tao L, Chao J, Huo F. A near infrared turn on fluorescent probe for biothiols detection and its application in living cells. Sens Actuators B Chem 2017;246:988–93.
[78] Yue Y, Huo F, Li X, Wen Y, Yi T, Salamanca J, Escobedo JO, Strongin RM, Yin C. pH-dependent fluorescent probe that can be tuned for cysteine or homocysteine. Org Lett 2016;19:82–5.
[79] Jiang Z, Liu Y, Hu X, Li Y. Colorimetric determination of thiol compounds in serum based on Fe-MIL-88NH_2 metal organic framework as peroxidase mimetics. Anal Methods 2014;6:5647–51.